Behavioral Modeling of Microtweezer Integrated with Capacitive Touch Sensor

Nayyer Abbas Zaidi[#1], Shafaat A. Bazaz[#2], Nisar Ahmed[#3], Rahim Umar[#4]
[#1#,3] Faculty of Electronic Engineering, Ghulam Ishaq Khan Institute of Engineering Sciences and Technology, Pakistan.
[#2]Department of Computer Science, Centre for Advance Studies in Engineering (CASE), 19 Ataturk Avenue, G-5/1, Islamabad, Pakistan.
[#4] Faculty of Engineering Sciences, Ghulam Ishaq Khan Institute of Engineering Sciences and Technology, Pakistan.
E-mail: nayyergiki@gmail.com

Abstract: This paper presents behavioral modeling of an electrostatic microtweezer integrated with capacitive touch sensor. The design of the microtweezer is optimized using standard SOIMUMPS process. Microtweezer performance is forecasted using system level simulation. The results of the system level simulation obtained from behavioral modeling shows total displacement of 7.039 µm and 37.5 µm is obtained at central beam and tweezer jaw respectively, when a voltage of 55 V is applied. Behavioural modeling of the sensor part of microtweezer is performed and system level simulation results shows that minimum and maximum capacitance is 0.45 pF and 0.65 pF respectively. Pull-in voltage analysis through behavioral modeling shows that actuator works with maximum performance, at applied voltage of 55 V. The results of displacement, sense capacitance and pull-in voltage analysis are nearly identical to analytical results when compared.

Keywords: MEMS, Behavioural model, SOIMUMPS, System level simulation, Microtweezer..

1. Introduction

In the last ten years, new customized as well as standard micromachining processes have been emerged, making it possible to develop complex type of Microelectromechanical systems (MEMS). Due to such innovations, MEMS have found its place in many practical applications where one of the areas is micromanipulation of micro-objects. Micromanipulation has become important in the applications, like microassembly, to assemble parts of micron size that are generally fabricated on a substrate. One such micromanipulator was developed in 2004, that uses MEMS microtweezer as an end-effecter attached to the robotic workstation [1]. The microtweezer performs the task of grasping the micropart and then the robotic arm performs the manipulation operation. A passive microtweezer is designed to grasp the micro-object with a specific size. Another important application of micromanipulator is in the area of biological and biomedical research [2]. Design of three degree-of-freedom Micromanipulator based on MEMS heat actuators have been developed that can

Received: 4 August 2013 / Accepted: 8 April 2014

© 2014 CMSIM
ISSN 2241-0503

be used to probe or position biological object [3]. Another three degree-of freedom micromanipulator based on comb drive actuators were developed for precise positioning of probing instruments like Atomic Force Microscopy (AFM), or tools to provide energy beam like e-beam, X-ray etc. [4]. These systems cannot safely grasp the micro-objects. Moreover, all such systems do not provide integrated sensing mechanism that makes their use to limited applications.

Many MEMS based microtweezers have been proposed in recent years for different micromanipulation applications [2, 5, 6]. Most of these microtweezers were based on electrostatic or piezoelectric actuation principle. These microtweezers comprised of the jaws mechanism with the dimensions of the size of the cell that are generally of diameter of tens of microns. Moreover, these jaws should be able to grasp the cells with different and irregular shapes. In order to grasp more precisely, not only the jaw mechanism but also the integration of touch sensor, makes microtweezer design more effective. As this addition excludes the fracture of microobject due to the uncontrolled excessive force, which is not found in to the microtweezers design proposed by Kim and Volland [5, 6]. Finally, batch production of such system requires the use of standard MEMS based micromachining technology thus making it cost effective, have good repeatability and also reliability from the point of view of the fabrication and production of the microstructures.

To fabricate microtweezer, Modeling and Simulation plays vital role in predicting the dynamics of the device. These analytical and simulation results minimizes iterative fabrication that is costly and time consuming. Previously microtweezers were simulated using Finite Element Methods [2, 3, 19, 20]. Beside the fact that, these methods gave high accurate solution but a compromise is made in terms of times, memory requirement and the restriction of integration of electronics with the device, bounded the user to limited type of simulations.

On the other hand, Behavioral Modeling and system level simulation tool performs MEMS analysis efficiently both in terms of time, memory requirement and integration of electronics with the MEMS makes Microsystem to be analyzed in a single simulation environment. In mid-nineties, simulation tools such as SUGAR and NODAS that comprise basic MEMS elements library were developed at UC Berkeley and Carnegie Mellon University respectively, in which Matlab and Cadence are used as system level simulator [7, 8, 9]. Now days, very specialized MEMS modeling and simulation such as CoventorWare Architect [17] with large MEMS library is available to simulate MEMS devices. Various MEMS devices including Gas Sensors [10], Accelerometers [11] and Gyroscope [12] were first simulated in CoventorWare Architect and then they are fabricated.

This paper presents the analytical analysis of microtweezer with its novel behavioral modeling and simulation of both the actuator and the sensor part. In Section II, SOIMUMPs process is explained, in which sample model of the

microtweezer is designed. In section III, design details of microtweezer are explained. The theory of operation of microtweezer is explained in section IV. The parameters related to design such as displacement, change in capacitance and pull in voltage are discussed in section V. The behavioral modeling is illuminated in section VI and then results and discussion in section VII. Finally section VIII illustrates conclusion.

2. SOI-MUMPS Process

The standard SOI-MUMPs [13] process is selected for the development of sample model of microtweezer. The reason for choosing this process is, it is easily available with reliable design instructions. SOIMUMPs process offers, 2 µm minimum feature size and spacing between structure layers. This can be used to construct a high capacitance com drive. In order to grasp a microobject through microtweezer the grasping area should be equal or larger then the thickness of the micro-object. This process proposes quite high grasping area of 25 µm, which is enough to grasp a microobject. The fabrication sequence of the microtweezer using SOIMUMPs process is shown in Fig. 1.

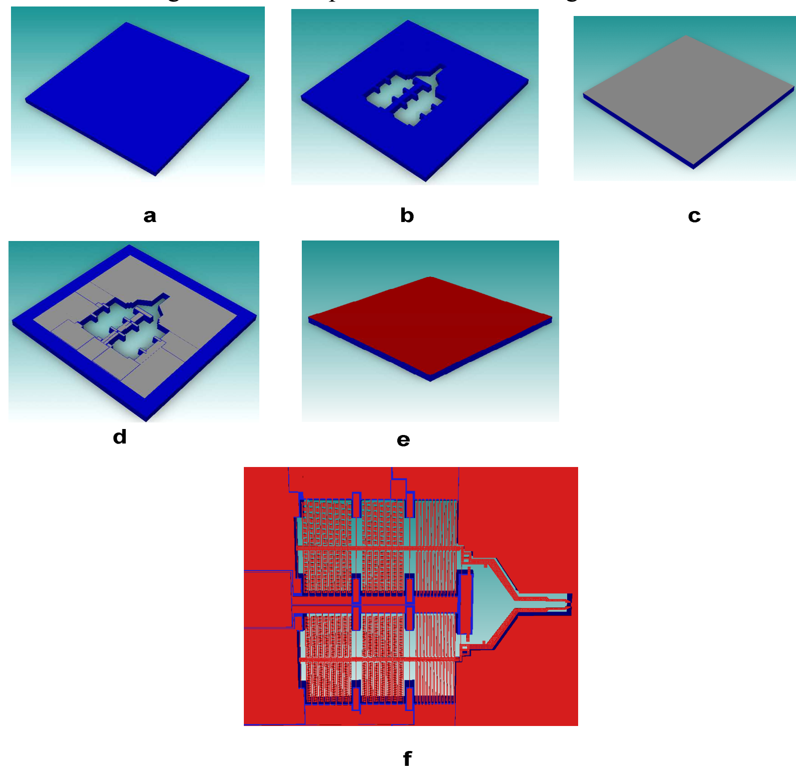

Fig. 1: Process flow for the fabrication of microtweezer using SOI-MUMPS in CoventorWare.(a)Silicon-on-insulator (SOI) wafer as starting substrate (b)DRIE silicon etch is used to etch substrate completely (c) Thermal

oxidation is done to built insulator layer on substrate (d) DRIE etch completely etch the substrate and oxide layer (e)Single crystal silicon layer is deposited having thickness of 25um (f) Deep reactive ion etch is used to etch the silicon to the oxide layer and after that finally DRIE is used to etch down to the oxide layer.

3. Microtweezer design

The designed microtweezer 2-D layout, developed in MEMSPro is shown in Fig. 2. It consists of three parts a) actuator b) sensor and c) jaws.

3.1 Actuator Design

The actuator part of the microtweezer is comprised of comb drive mechanism which is Lateral. This technique consists of interdigitated finger, in which fixed and moveable parts are called stator and rotor combs. The length of the fingers is set to 50 µm and overlap length is set to 30 μm. The spacing between the two fingers is designed to 3 μm to avoid the collapse of the fingers as shown in Fig. 3. The three clamped-clamped beams are used to suspend the structure and moves back the central mass movement to its free position.

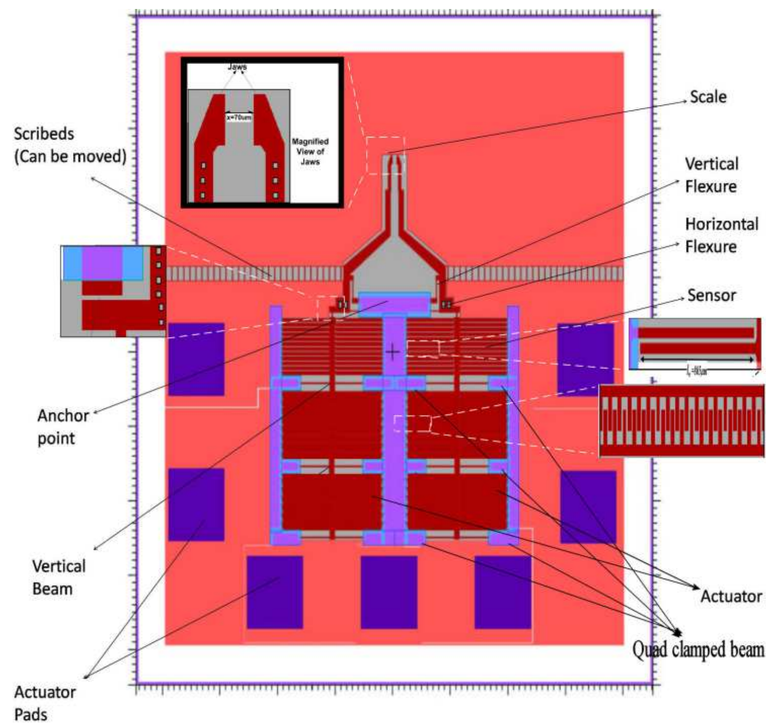

Fig. 2: Complete microtweezer design with integrated touch sensor.

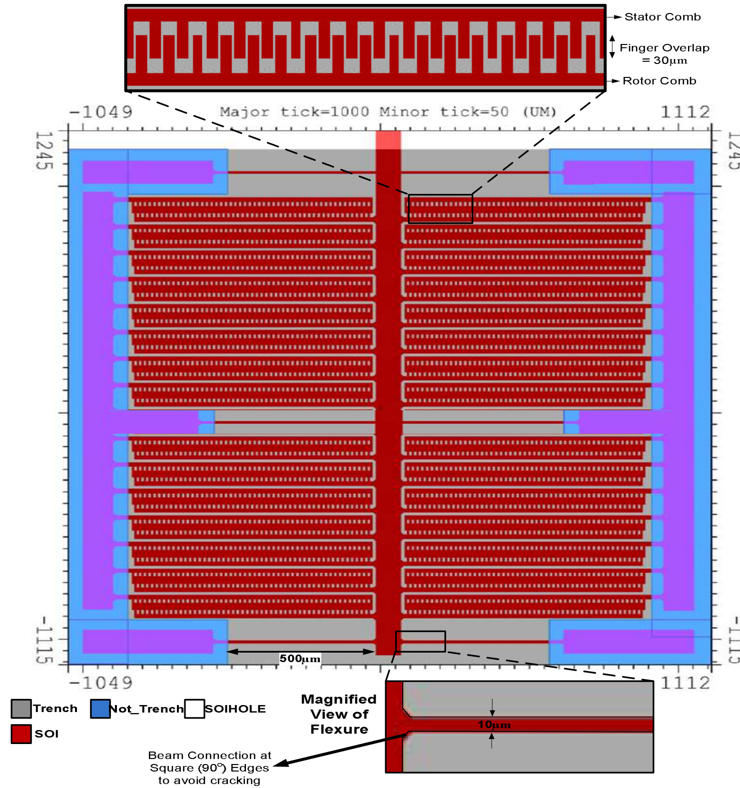

Fig. 3: Complete actuator design.

3.2 Sensor design

Differential transverse comb based touch sensor is designed to sense the touch when the object gripped between the tweezer jaws. The working principle of the sensor comb are, up on the application of the force applied to the moveable combs attached with the central mass cause the increase in the finger gap on one side of the microtweezer and decrease the same amount of gap on the other side of the moveable combs as shown in fig. 4. The overlap length and gap between the sensor fingers are 805 µm and 10 µm respectively and of the width of fingers is 25 µm.

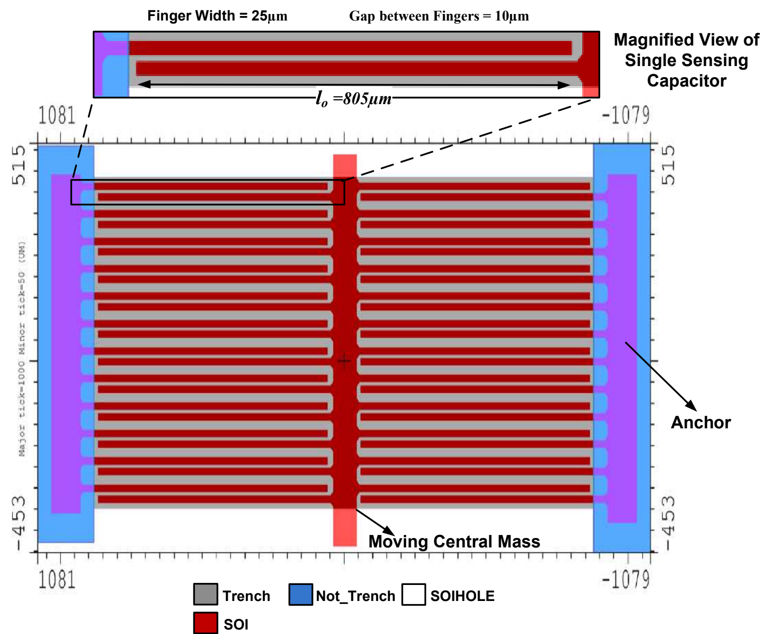

Fig. 4: Complete sensor combs design.

3.3 Jaw Design

A novel tweezer arm and jaw with the compliant structure has been designed as shown in Fig. 5 for grasping the micro-sized objects. The design includes a horizontal and a vertical beam to produce elastic restoring force in horizontal and vertical direction simultaneously. The vertical beam additionally provides support against the out of plane movement of the tweezer arms. The structure is designed in such a way that it will maintain an angle of 90^0 between the tweezer arm and the horizontal beam. Additionally, the jaw moves a little distance forward along *y*-axis during grasping due to direction of applied force. This action ensures that object completely comes between the jaws while grasping. Two stoppers have been placed near the point of application of force in order to stop any extra movement of central beam after the object has been fully grasped. In the proposed tweezer arm design, the vertical displacement produced in central beam is amplified by constant times the displacement produced at the tips of tweezer jaws.

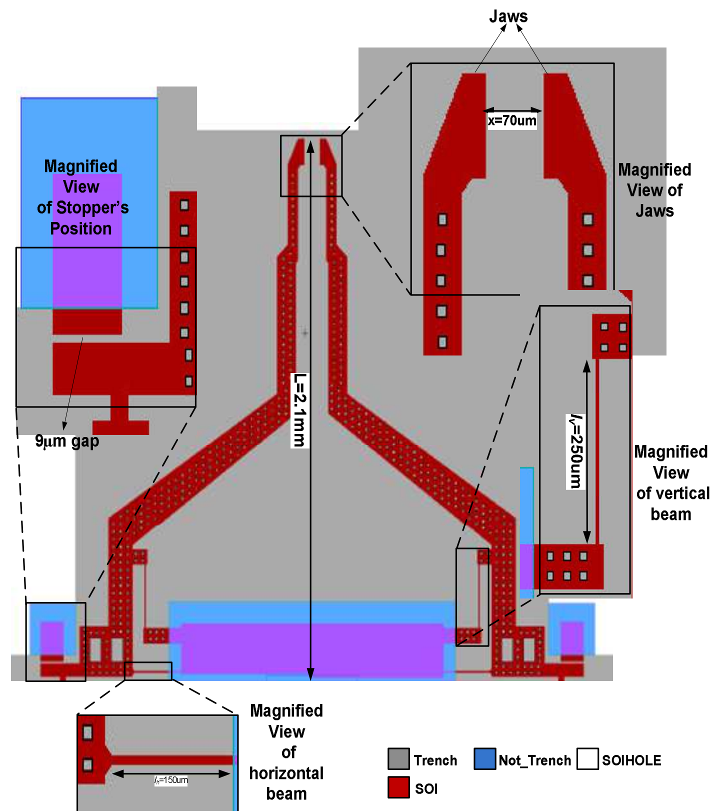

Fig. 5: Complete design of tweezer arms.

4. Theory of operation

The proposed microtweezer design uses novel dual electrostatic actuation system i.e. there are two separate electrostatic actuators for the simultaneous movement of two jaws. Each actuator consists of a set of stator combs interdigitated with a set of rotor combs. DC voltage is applied to both the actuators simultaneously such that the stator combs are at positive potential with respect to rotor combs. Hence electrostatic force is produced which pulls the two comb drives. This electrostatic attraction produces elastic restoring force in the quad clamped flexure springs which is equal in magnitude to the applied force. The central beam of each actuator is attached to the respective tweezer arm. Each tweezer arm is further supported by two cantilever beams namely horizontal and vertical beam. Hence total elastic restoring force is a combination of force due to the quad-clamped flexure springs and the two cantilever beams. Any vertical movement of the central beam in upward direction is amplified at the tweezer jaws due to the integrated action of the tweezer arm and the beam

system. One transverse comb drive based capacitive touch sensor is included along each of the two central beams in between the tweezer arm and actuator explain in Fig. 2. The overlap length varies in the sensor combs result in the change in capacitance. When there is no capacitance change it indicates that the object has been gripped and thus to avoid any damage to the object no further actuation voltage is applied.

5. Design parameters

5.1 Displacement of central beam

An applied voltage to actuator generates electrostatic force between the comb drives. This electrostatic force is conveyed to the jaw via quad-clamped, horizontal and vertical flexures. The spring constant of flexures added because of parallel connection [15].

$$K = k_h + k_f + k_v \quad (1)$$

$$K = Et\left(\frac{8b_f^{3}}{l_f^{3}} + \frac{b_h^{3}}{4l_h^{3}} + \frac{b_v^{3}}{4l_v^{3}}\right) \quad (2)$$

Using Hook’s law force in terms of displacement is given as:

$$F = Et\left(\frac{8b_f^{3}}{l_f^{3}} + \frac{b_h^{3}}{4l_h^{3}} + \frac{b_v^{3}}{4l_v^{3}}\right) \text{ EMBED Equation.3 } y \quad (3)$$

The electrostatic F produced by actuator is given as:

$$F = \frac{N.n}{2}\varepsilon\frac{tV^{2}}{d} \quad (4)$$

Where nN is the entire number of comb drives connected in parallel, t is the thickness, d is the gap between the comb drives and V is the applied voltage. Eq. (3) and (4) are equated, the central mass displacement is given as:

$$\mathbf{y} = \frac{\frac{N.n}{2}\varepsilon_o\frac{tV^{2}}{d}}{Et\left(\frac{8b_f^{3}}{l_f^{3}} + \frac{b_h^{3}}{4l_h^{3}} + \frac{b_v^{3}}{4l_v^{3}}\right)} \quad (5)$$

5.2 Displacement of single Jaw

The horizontal flexure and the length of the jaw are responsible for the amplification at the jaws. Thus central beam movement is amplified by L/L_Q. The total movement at single jaw is calculated as:

$$\mathbf{X} = \frac{L}{l_Q} \text{▯ EMBED Equation.3 ▯▯▯} \frac{\frac{N.n}{2}\varepsilon\frac{tV^2}{d}}{Et\left(\frac{8b_f^3}{l_f^3}+\frac{b_h^3}{4l_h^3}+\frac{b_v^3}{4l_v^3}\right)} \quad (6)$$

Where $L=2.1mm$ is the length of the microtweezer jaws and $l_Q = 150\ \mu m$ horizontal flexure length as shown in Fig. 5.

5.3 Sensor

In the sensor, the capacitance increases and decreases by same proportion on the two sides of the comb drives. These capacitances are given as:

$$\left.\begin{aligned} C_{s1} &= Nn\frac{\varepsilon(t \times l)}{d_0 + \left(\frac{L}{L_Q}\right)X} + C_{fringe} \\ C_{s2} &= Nn\frac{\varepsilon(t \times l)}{d_0 - \left(\frac{L}{L_Q}\right)X} + C_{fringe} \end{aligned}\right\} \quad (7)$$

where d_0 is the initial gap between the transverse combs, C_{s1} is the decreased capacitance and C_{s2} is the increased capacitance in the transverse comb sensor corresponding to the gap change $y = \left(\frac{L}{L_Q}\right)X$ and C_{fringe} is the capacitance produced due to the fringe fields.

5.4 Pull-in Voltage

In the proposed microtweezer design, the comb drive actuator one of which, typically called as rotor finger, is suspended and connected to the compliant springs while other, usually called as stator finger, is fixed. The pull in voltage is defined as the voltage at which the two fingers come in touch with each other. The pull-in voltage $V_{pull-in}$ is given [16]:

$$V^2_{pull-in} = \frac{d^2 k_y}{2\varepsilon_0 bn}\sqrt{2\frac{k_x}{k_y} + \frac{y_0^2}{d^2}} - \frac{y_0}{d} \quad (8)$$

Where d is the gap spacing between the fingers, ε_o is the dielectric constant in air, $\frac{k_x}{k_y}$ is the spring stiffness ratio.

6. Behavioural model development

The reduced order equations are used to perform behavioral modeling and simulation. In this modeling technique complete model is simulated rather than simulating number of finite components that constitute the model. Thus the efficiency in time is achieved in this method rather than finite element analysis. The components that are used to develop behavioral model are presents in its libraries. The core code inside these libraries tells the individual components how to behave when exposed to stimuli in terms of electrical and mechanical [17]. The main components that develop behavioral model design are Beams, Comb drives and rigid plates. Fig. 6 shows the behavioral schematic of the actuator, sensor and jaw. Mechanical bus is used for connecting the components. This bus consists of array of six wires in which three are translational and other rotational. These wires contain information about rotational and translational motion of the mechanical components in space. The mechanical bus connector is connected at the tip of the jaw and with central beam in order to find their displacement. The 3-D model shown in Fig. 7 is generated after net listing and importing the schematic design in to scene 3D of the architect. In the 3D model half portion of the microtweezer is modeled because of geometrical evenness.

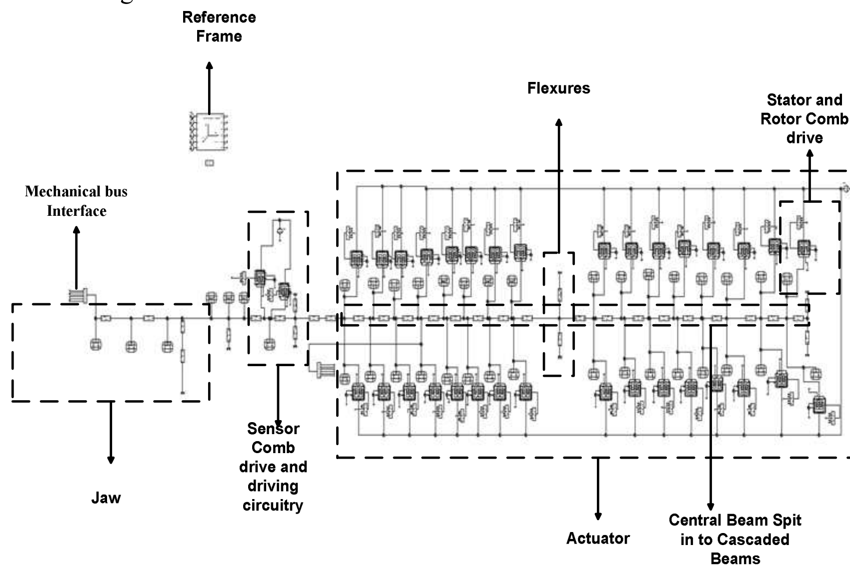

Fig. 6: Behavioural schematic of the microtweezer.

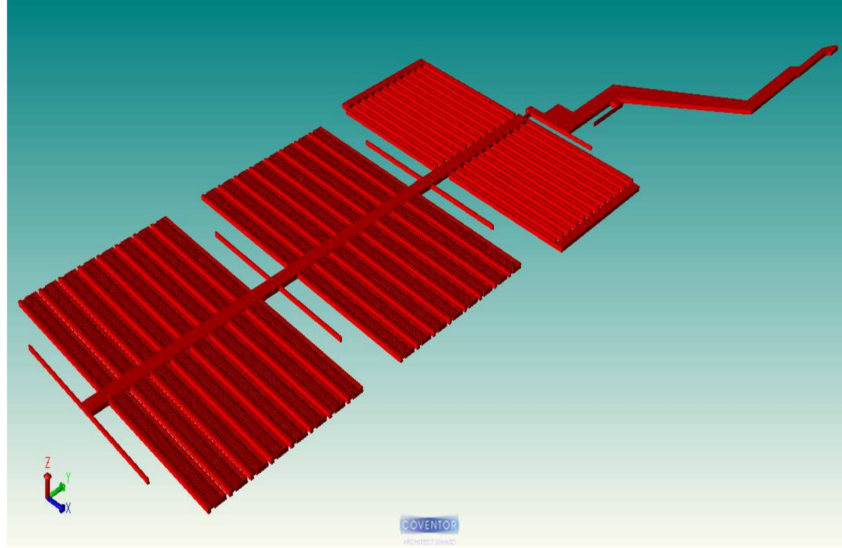

Fig. 7: Microtweezer 3-D model in CoventorWare architect.

7. Result & discussion

The graph shown in Fig. 8 obtained analytically (by Eq. (5)) for a displacement of central beam when a voltage is sweep form 0 - 55 V. At 50 V the displacement is found to be 6.3 μm. The behavioral model simulation, between voltage and central beam displacement is shown in Fig. 9. Both the results are approximately same as analytically predicted. The simulation results are shown in Fig. 10, the color of the contours plot shows the displacement of every component of the microtweezer in *y*-axis direction. It is observed that stator combs are stationary while rotor combs moves the central beam in *y*-axis.

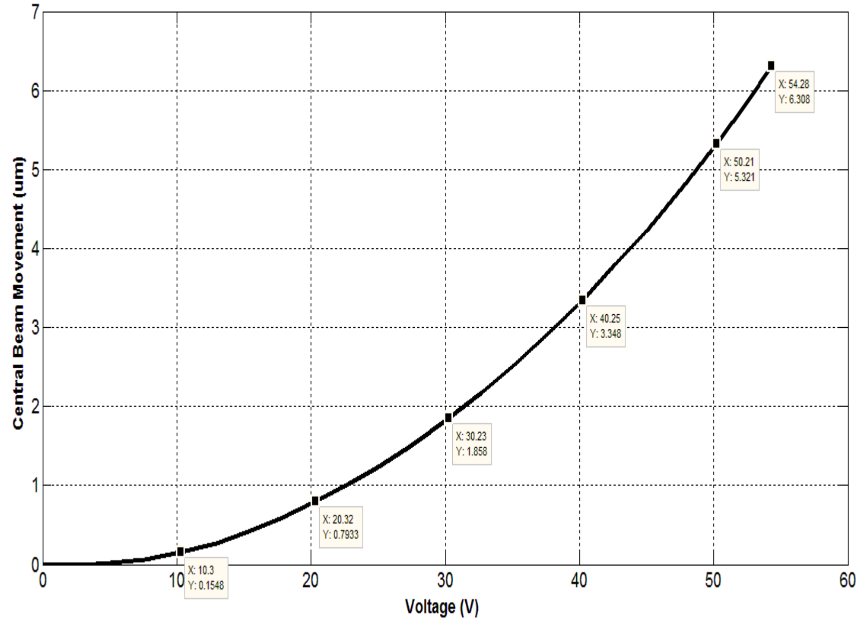

Fig. 8: Analytical relation between voltage (V) and central beam displacement (µm).

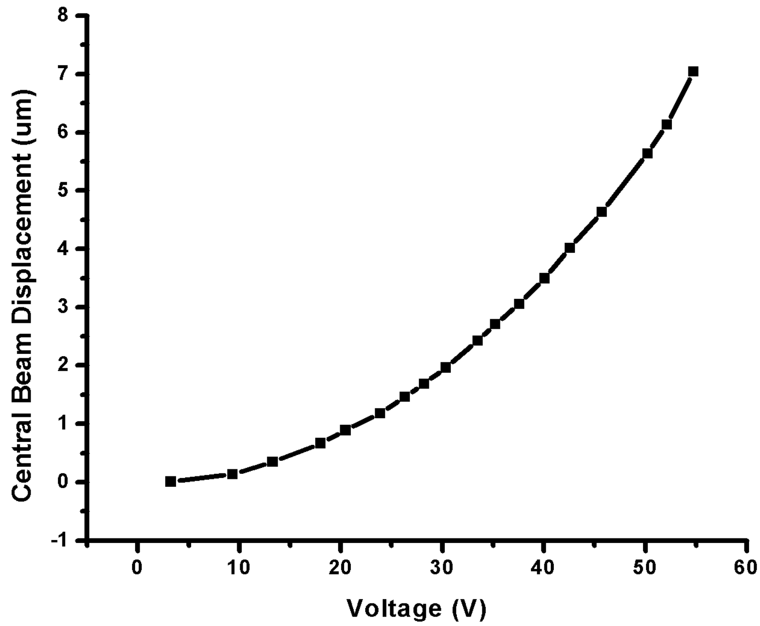

Fig. 9: Graph between voltage (V) and central beam displacement (µm) acquired by behavioral modeling.

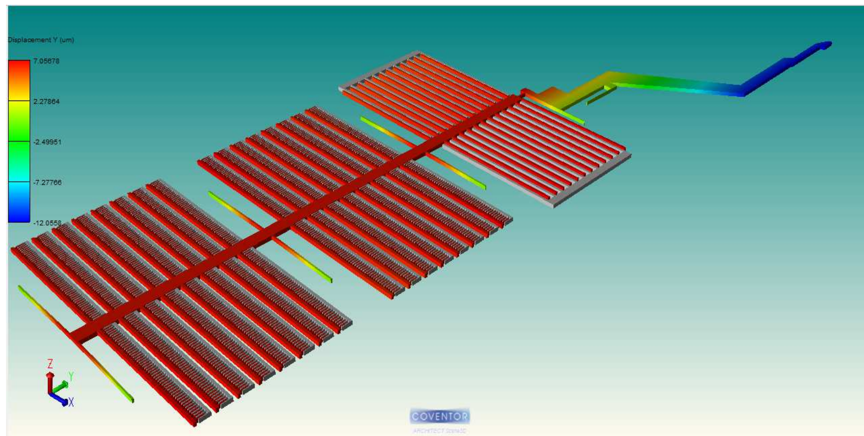

Fig.10: Displacement visualization in a color contours for microtweezer.

The graph shown in Fig. 11 is the analytically calculated result that is obtained from Eq. 6, between voltage (V) and the jaw displacement (μm). The maximum displacement obtained is at the tip of the jaw which is 34.3 μm at 55 V. The jaw displacement obtained through system level simulation is 38 μm at 55 V which is nearly same as analytically calculated. From analytically and simulation outcomes show that the microtweezer can easily grasp microobjects in diameter from 0 – 70 μm when it's both jaws are in motion. This can avoid the fabrication of 2 stage jaws [18].

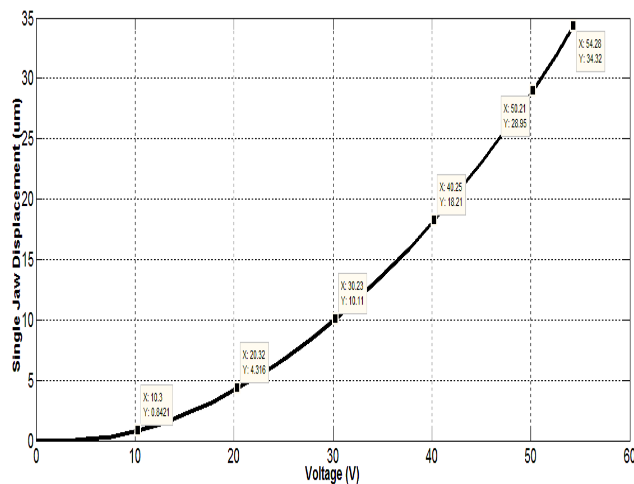

Fig. 11: Analytical relationship between voltage (V) and jaw displacement (µm).

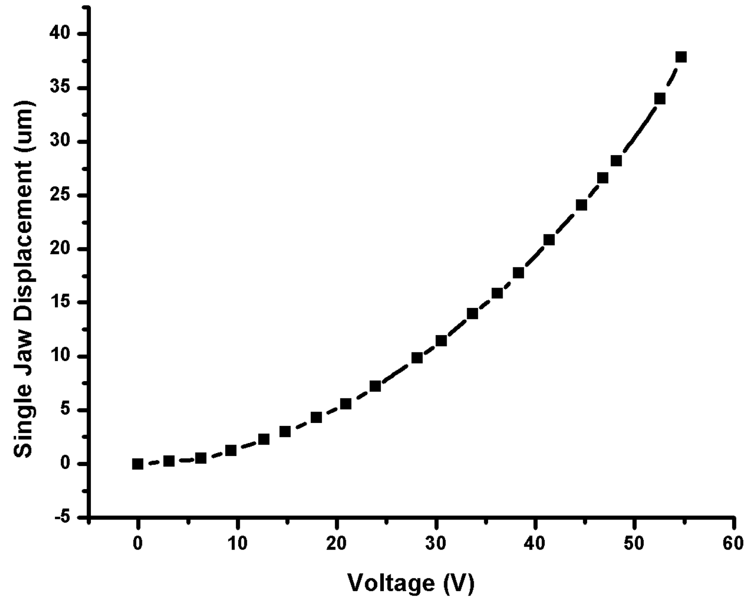

Fig. 12: Graph between voltage (V) and jaw displacement (µm) obtained by behavioral modeling.

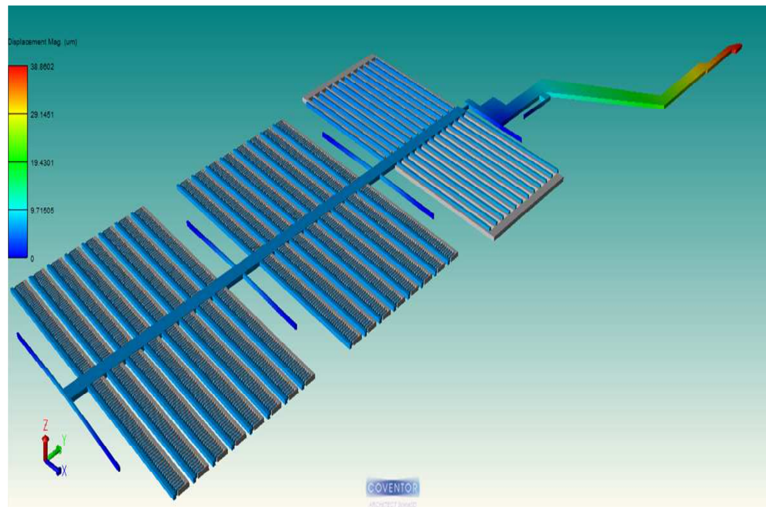

Fig. 13: Displacement visualization in a color contours for microtweezer.

The graph shown in Fig. 14 and Fig. 15 shows the change in capacitance vs displacement of transverse comb drive calculated both analytically by Eq. (7), and over behavioral modeling respectively. Form the result it is clear the capacitance on one side of the transverse C_{S1} increases while the capacitance on

the other end C_{S2} decreases. The behavioral model result shows the same capacitance increase and decrease. These results are approximately the same. The integration of the capacitive touch sensor informs that the range of capacitance (0.45 *f*F - 0.65 *f*F) that is obtained in gripping microobject. This range of capacitance is significant in programming the capacitive read out circuitry MS3110 [14].

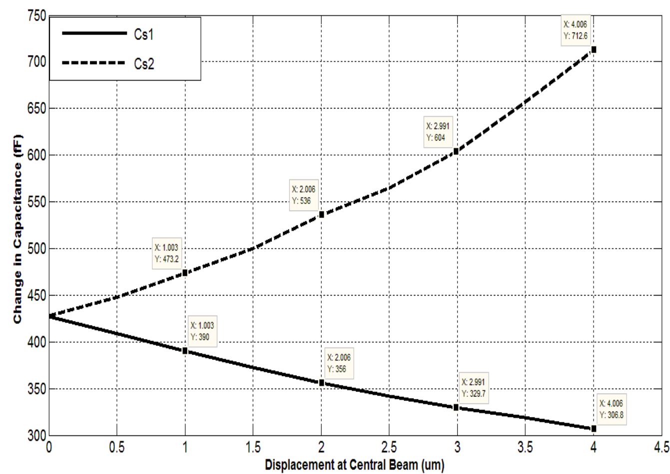

Fig. 14: Analytical relationship between displacement at central beam and change in capacitance (fF).

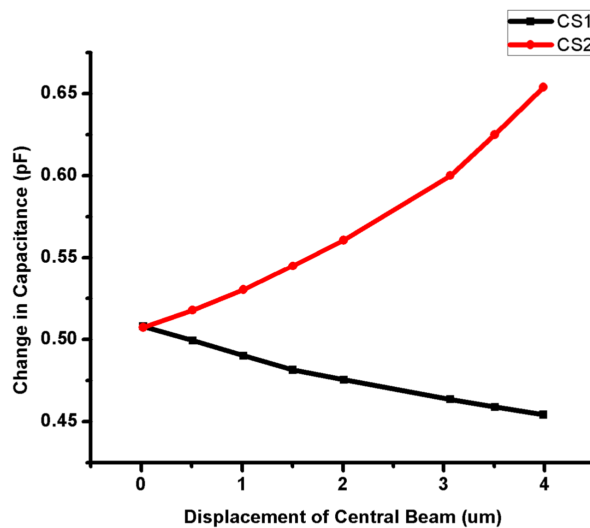

Fig. 15: Graph between displacement at central beam and change in capacitance (fF) obtained by behavioral modeling.

The pull in voltage analysis is carried out to predict the maximum operating voltage of the actuator of the microtweezer. Analytically the maximum pull in voltage calculated through Eq. 8 is 55 V while through system level simulation 58 V is obtained. These results are approximately same.
The above defined parameters are summarized in Table:1, which reveals that the possibility of developing a prosperous device are higher because of the fact that the analytical and behavioral models results are nearly equal.

Parameter	Analytical results	Behavioral model results
Maximum Central Beam moment (μm)	6.3	7.039
Maximum Jaw Displacement (μm)	34.3	38
Capacitance (fF)	C_{s1}: 306fF C_{s2}: 712fF	C_{s1}: 0.45pF C_{s2}: 0.65pF
Pull-in voltage (V)	0 - 55	0 - 58

Table 1: Comaprison between analytical and behavioral model results.

8. Conclusions

A MEMS based microtweezer integrated with capacitive touch sensor has been designed using SOI-MUMPS process. The layout model of the device is developed in MEMSPro CAD tool environment. The designed microtweezer gives analytically central beam displacement of 6.3 μm, single jaw displacement of 7.03 μm, capacitance change of C_{S1}=306 fF and C_{S2}=712 fF and result of pull-in voltage is 55 V.
Extensive simulation through behavioral modeling using the architect module of the CoventorWare verifies the maximum central beam movement of 7.03 μm and jaw displacement of 38 μm with change in capacitance of 0.45pF to 0.65pF. Pull-in voltage analysis shows that at 58 V, actuator gives maximum performance. The use of analytical and simulation approach avoids iterative fabrication that is expensive. The microtweezer is now ready to send for fabrication with higher chances of its success.

References

[1] N. Dechev, W.L. Cleghorn, and , J.K. Mills, "Microassembly of 3D microstructures using a compliant, passive microgripper", *Journal of Microelectromechanical Systems,* Vol. 13, No. 2, pp. 176-189, 2004.

[2] T. Chen, L. Chen, and L. Sun, "Pizeoelectrically driven silicon microgripper integrated with sidewall piezoresistive sensor", *Proceedings of the IEEE International Conference on Robotics and Automation*, Kobe, Japan, pp. 2989-2994, 2009.

[3] S. Venugopal, L.C. Jsu, S.M.N. Rao, B.P.Wang, M. Chiao, and J.C. Chiao, “Design and modeling of a high accuracy, three degree of freedom MEMS manipulator”, *Conference on MEMS and Photonics*, Brisbane, Australia, 2005.

[4] B. R. Jong, D. M. Brouwer, M. J. Boer, H. V. Jansen, H. M. J. Soemers, and G. J. M. Krijnen, “Design and fabrication of a planar three-DOFs MEMS-based manipulator”, *Journal of Microelectromechenical System*, Vol. 19, No. 5, pp. 1116-1130, 2010.

[5] C. J. Kim, A. P. Pissano, and R. S. Muller “Silicon-processed overhanging microgripper”, *Journal of Microelectromechenical System*, Vol. 1, No. 1, pp. 31–36, 1992.

[6] B. V. Volland, H. Heerlein, and I. W. Rangelow, “Electrostatically driven microgripper”, *Journal of Microelectronic Engineering*, Vol. 61 , pp. 1015-1023, 2002.

[7] J. V. Clark, N. Zhou, S. Brown and K. S. J. Pister, “MEMS Simulation Using SUGAR v0.5”, *Solid-State Sensors and Actuators* pp. 191-196, 1998.

[8] Q. Jing, T. Mukherjee and G. K. Fedder, “Schematic-Based Lumped Parameterized Behavioral Modeling for Suspended MEMS”, *International Conference on Computer Aided Design, San Jose*, CA, Nov. 10-14, 2002.

[9] G. C. Wong, G. K. Tse, Q. Jing, T. Mukherjee, G. K. Fedder, “Accuracy and Composability in NODAS”, IEEE Int. Workshop on Behavioral Modeling and Simulation, San Jose, CA, 2003.

[10] G. Uma, M. Umapathy, L. Baby Vidhya, M. Maya, T. Sophia and K. Tamilarasi, “Design and Analysis of Resonant Based Gas Sensor”, *Sensors Applications Symposium*, Atlanta,. pp 119-121, 2008.

[11] A. Manut and M. I. Syono “Effects of Mechanical Geometries on resonance Sensitivity of MEMS Out-of-Plane Accelerometer”, *IEEE International Conference on Semiconductor Electronics*, Kuala Lumpur, 2006.

[12] Kashif Riaz, Shafaat A. Bazaz, M. Mubasher Saleem and Rana I. Shakoor, “Design, Damping Estimation and Experimental Characterization of Decoupled 3-DoF Robust MEMS Gyroscope”, *Journal of Sensors and Actuators A.,* Vol. 172, No. 2, pp. 523-532, 2011.

[13] K. Miller, A. Cowen, G. Hames, B. Hardy, SOIMUMPs Design Handbook, Version 4, MEMSCAP Inc., 2004. Available at: http://www.memscap.com/products/mumps/soimumps/reference-material

[14] Universal Capactive Readout^{TM} IC (MS3110) manual Irvine Sensor Coropration. Available at: http://www.irvine sensors.

[15] M. Bao, “Analysis and design principles of MEMS devices” *1st edition Elsevier*, 2005.

[16] R. Legtenberg, A. W. Groeneveld and M. Elwenspoek, “Comb-drive actuators for large displacements”, *Journal of Micromechanics Microengineering*, Vol. 6, No. 3 pp. 320-329, 1996.

[17] CoventorWare ARCHITECT, version 2008, Reference: MEMS and Microsystems System-Level Design Coventor, Inc.

[18] K. Amjad, S. A. Bazaz and Y. Lai, “Design of an electrostatic MEMS microgripper system integrated with force sensor”, The *20th IEEE international conference on microelectronics*, Sharjah, 2008, pp 275–278, 2008.

[19] F. Krecinic, T.C. Duc, G.K. Lau and P.M. Sarro “Finite element modeling and experimental characterization of an electro-thermally actuated silicon-polymer microgripper”, Journal of micromechanics and Microengineering, Vol. 18, pp., 2008.

[20] E.V. Bordatchev and S.K. Nikumb, “Microgripper: Design, finite element analysis and laser microfabrication”, proceeding of the international conference on MEMS, NANO and Smart Systems, Canada, pp. 308-313, 2003.